Neurocomputing 529 (2023) 113–127

Contents lists available at ScienceDirect

Neurocomputing

journal homepage: www.elsevier.com/locate/neucom

Comparison of spiking neural networks with different topologies based on anti-disturbance ability under external noise

Lei Guo [a,b,*], Dongzhao Liu [a,b], Youxi Wu [c], Guizhi Xu [a,b]

[a] State Key Laboratory of Reliability and Intelligence of Electrical Equipment, Hebei University of Technology, Tianjin 300130, China
[b] Hebei Key Laboratory of Bioelectromagnetics and Neural Engineering, School of Health Sciences and Biomedical Engineering, Hebei University of Technology, Tianjin 300130, China
[c] School of Artificial Intelligence, Hebei University of Technology, Tianjin 300401, China

ARTICLE INFO

Article history:
Received 30 July 2022
Revised 6 December 2022
Accepted 30 January 2023
Available online 2 February 2023
Communicated by Zidong Wang

Keywords:
Spiking neural networks
Complex network topology
Synaptic plasticity
Anti-disturbance ability
Speech recognition

ABSTRACT

The research on robustness of brain-like models contributes to promoting its neural information processing ability, and the understanding of bio-brain function. However, the biological rationality of the current brain-like models is inadequate. In addition, the effect of network topologies on the robustness of brain-like models has not been clarified. In this study, inspired by the topological characteristics of biological functional brain networks, we construct five kinds of spiking neural networks (SNNs), which have the same Izhikevich neuron model and the same synaptic plasticity model with time-delay, but different network topologies. Then, the robustness of the SNNs with different topologies is comparatively assessed based on the anti-disturbance ability under different noise. Further, by taking a speech recognition task as the case study, we investigate the anti-disturbance ability of these SNNs in application. Finally, the anti-disturbance mechanism of the SNNs is discussed. Our simulation consistently certifies that: (i) In terms of anti-disturbance indicators, the complex SNN outperforms the small-world SNN, the small-world SNN outperforms the scale-free SNN, and all of them outperform the random SNN and the regular SNN, which indicates that the SNNs with more biological rationality have the better anti-disturbance ability. (ii) In terms of speech recognition accuracy, the performance of SNNs with different topologies presents the consistent order with the anti-disturbance ability above. And the recognition accuracy of these SNNs under disturbance still remains almost the same, compared with these SNNs without disturbance. (iii) The evolution process of neural information is clarified, which hints that the synaptic plasticity is the intrinsic factor of anti-disturbance ability, and the network topology is a factor that affects the anti-disturbance ability at the level of performance. Our simulation results are conducive to the design of neuromorphic algorithms with robustness on analog or mixed-signal neuromorphic chips under complex noise environment.

1. Introduction

The integration of neurosciences and artificial intelligence is conducive to improving the biological rationality and the neural information processing ability of brain-like models. The bio-brains have self-adaptive abilities, including self-learning, self-organization, and self-repairing [1–3]. Inspired by the self-adaptive abilities of bio-brains, the construction of brain-like models with more biological rationality has become the frontier. Meanwhile, the research on neural information processing in a brain-like model in turn promotes the understanding of bio-brain function. However, the biological rationality of the current brain-like models is inadequate. The spiking neural network (SNN) is the latest generation of artificial neural network model [4], which can well reflect the electrophysiological characteristics of biological neuronal networks. SNNs under the regulation of neuronal dynamics and synaptic weight dynamics can process complex nonlinear spatio-temporal information, which makes it an important model basis in the field of brain-like intelligence [5–7]. The three components of constructing an SNN are neuron model, synaptic plasticity model, and network topology.

The neuron model is the elemental unit of information processing in an SNN, which reflects the electrophysiological characteristics of bio-neurons through the mathematical model. The

* Corresponding author at: State Key Laboratory of Reliability and Intelligence of Electrical Equipment, Hebei University of Technology, Tianjin 300130, China; Hebei Key Laboratory of Bioelectromagnetics and Neural Engineering, School of Health Sciences and Biomedical Engineering, Hebei University of Technology, Tianjin 300130, China.
E-mail address: guolei@hebut.edu.cn (L. Guo).

https://doi.org/10.1016/j.neucom.2023.01.085
0925-2312/

Hodgkin-Huxley neuron model, as a fourth-order ordinary differential equation, can be well consistent with the firing characteristics of bio-neurons and accurately describe the changes in membrane potential [8]. However, the high computational cost makes it difficult to be applied in large-scale networks. Conversely, as a first-order ordinary differential equation, the Leaky Integrate-and-Fire (LIF) neuron model has low computational cost, but is inadequate in reflecting the firing characteristics of bio-neurons [9]. The Izhikevich neuron model simplifies the Hodgkin-Huxley neuron model into a second-order ordinary differential equation by bifurcation method, which makes the Izhikevich neuron model significantly reduce the computational cost while simulating the firing characteristics well of bio-neurons [10]. Therefore, the Izhikevich neuron model is widely applied to construct SNNs [11–13].

The synapse is the material foundation of neural information interaction among neurons. The excitatory synapse can enhance the interaction efficiency of neural information [14]. Meanwhile, the inhibitory synapse dynamically regulates neural information interaction in terms of efficiency, stability, and sensitivity, which forms the foundation of neural information interaction together with the excitatory synapse [15,16]. Drawing from the results of biological synapses, the synaptic plasticity model co-regulated by excitatory synapse and inhibitory synapse has been applied in brain-like models [17]. Diehl and Cook [18] investigated unsupervised learning of digit recognition based on a fully-connected SNN including excitatory synapses and inhibitory synapses, and demonstrated that the lateral inhibition of inhibitory synaptic plasticity is conducive to preventing the decline in recognition accuracy caused by excessive growth of synaptic weights. The diffusion of neurotransmitters in biological synapses with concentration gradient forms a synaptic time-delay in neural information interaction, which can improve the information processing ability of nervous system, and profit the formation of advanced cognitive function [19]. The synaptic time-delay in bio-neurons randomly distributes within the scope of 0.1–40 ms [20]. To construct the brain-like models with more biological rationality, synaptic plasticity with time-delay is introduced into the SNNs. Zhang et al. [21] introduced the synaptic delay plasticity into a weight-based supervised learning rule in an SNN, and found that the trained spiking neurons have better learning accuracy and efficiency since they can accurately reproduce the expected spiking sequence, compared with the traditional synaptic weight learning method. However, its synaptic time-delay depends on the distance between the expected spike output moment and the maximum spike input moment, which cannot accord with the dynamic scope of synaptic time-delay in bio-neurons. Therefore, the synaptic plasticity model according with synaptic time-delay in bio-neurons is an effective element that can improve the biological rationality in the construction of an SNN.

The network topology determines the connection form among nodes, and affects the function of an SNN. According to the topology structure, the networks can be divided into regular networks, random networks, and complex networks including small-world networks (SWNs) and scale-free networks (SFWs) [22]. Different topology structures have their own topological advantages. The regular network has a high average clustering coefficient (ACC), which means a high agglomeration degree of nodes [23]. The random network has a low average shortest path length (ASPL), which means a high global information transmission efficiency [24]. The SWN integrates the topological advantages of regular networks and random networks, which has the characteristics of high ACC and low ASPL [25]. The distribution of node degree in an SFN is extremely heterogeneous and conforms to a power-law distribution, which means a strong fault tolerance [26]. Cognitive neuroscience researches based on EEG, PET, or fMRI demonstrate that the biological functional brain networks are the SWNs and/or SFNs. Functional brain networks based on PET data from Dementia with Lewy bodies show that the ACC decreases and the ASPL increases, which means that the small-world property of the functional brain network in Dementia with Lewy bodies decreases, compared with the healthy controls [27]. Based on resting-state fMRI data in the frequency range related to the spontaneous neuroelectrical activity (0.01–0.1 Hz), the biological functional brain network has scale-free property, and its power-law index is related to the metabolic demand of brain regions [28]. Based on EEG data, the functional brain networks of alcohol addicts still have both small-world property and scale-free property. But the ACC decreases and the power-law index increases, compared with the topological characteristics of normal controls [29]. For small-world property, biological experiment results present the approximate range of functional brain networks in healthy humans, which is within the scope of [1.1, 2] [27,30–32]. For scale-free property, biological experiments indicate that the power-law index of human functional brain networks is about 2 [33–35]. The construction of SNNs inspired by biological functional brain networks has attracted focus. Neuronal firing patterns in a small-world SNN (SWSNN) indicate that the small-world property contributes to making electrical coupling more effective in inducing and enhancing the synchronous firing among neurons [36]. The neuronal firing synchronization in a scale-free SNN (SFSNN) indicates that changes in the degree distribution can make the SFSNN self-organize to the critical synchronization state [37]. According to the topological characteristics of biological functional brain networks, the complex SNN (CSNN) with both small-world property and scale-free property can improve the biological rationality of brain-like models.

The bio-brains respond to external stimulation through its self-adaptive regulation. Inspired by the self-adaption, scholars have focused on the response of brain-like models to external stimulation. Neuronal firing activity of SNNs indicated that synchronous firing patterns of neurons can be formed under the stimulation of white Gaussian noise [38]. The stochastic resonance phenomenon appears among neurons in an SWSNN under the electromagnetic radiation [39]. In previous work, we investigated the neural coding of an SFSNN under different external noise. Through the intra-type similarity and the inter-type specificity of neural coding, we certified that the SFSNN presented high neural coding specificity for different types of noise, which indicates that the SNN could differentiate the types of noise [40]. The research on synchronization, resonance and neural coding of SNNs can reflect the self-adaptive regulation of brain-like models to external stimulation. The robustness of brain-like models is another aspect of self-adaptive regulation. Saunders et al. [41] constructed a two-layer locally-connected SNN, and investigated its robustness through the damage of neurons or synapses. Their simulation results indicated that this SNN can maintain high accuracy on digit image recognition under the damage. However, cognitive neuroscience demonstrate that the biological functional brain networks are the SWNs and/or SFNs. In previous work, we discussed the robustness of SWSNNs and SFSNNs under targeted attack on neurons, and our results indicated that the SWSNN presented better anti-injury ability under the damage of high-degree neurons compared with the SFSNN [42]. Another perspective of robustness is anti-disturbance ability of brain-like models under external noise, which is conducive to developing neuromorphic algorithms with robustness under complex noise environment. Therefore, the purpose of this study is to investigate the robustness of SNNs with different topologies under external noise based on the anti-disturbance ability to obtain a brain-like model with better robustness. In this study, five kinds of SNNs with different topologies are constructed including CSNN, SWSNN, SFSNN, random SNN and regular SNN, in which the network nodes are presented by Izhikevich

neuron models, the network edges are presented by synaptic plasticity models with time-delay, respectively. Then, the robustness of these SNNs is comparatively assessed based on the anti-disturbance ability under different noise. Further, by taking a speech recognition task as the case study, we investigate the anti-disturbance ability of these SNNs in application. Finally, the anti-disturbance mechanism is discussed based on the evolution process of neural information. The main contributions of our study are as follows.

- To improve the biological rationality of brain-like models, a CSNN is constructed, in which the network nodes are presented by Izhikevich neuron models, the network edges are presented by synaptic plasticity models with time-delay, and the network topology is a small-world and scale-free network (SW-SFN) with both small-world property and scale-free property.
- To obtain the brain-like model with better robustness, the five kinds of SNNs are comparatively assessed based on two anti-disturbance indicators under three types of external noise. The simulation results consistently certify that the CSNN outperforms the SWSNN, the SWSNN outperforms the SFSNN, and all of them outperform the random SNN and the regular SNN in terms of anti-disturbance performance. Further, by taking a speech recognition task as the case study, we certify the anti-disturbance ability of these SNNs in application. These findings indicate that the brain-like models with more biological rationality have better robustness.
- To explore the anti-disturbance mechanism, the evolution process of neural information in the SNNs under external noise is clarified, which hints that the synaptic plasticity is the intrinsic factor of anti-disturbance ability, and the network topology is a factor that affects the anti-disturbance ability at the level of performance.

The rest of this study is organized as follows. The methods to construct SNNs with different topologies are provided in Section 2. The robustness of the SNNs with different topologies is comparatively assessed based on anti-disturbance ability in Section 3. The case study of speech recognition task is presented in Section 4. The anti-disturbance mechanism is discussed in Section 5. Finally, the conclusion is presented in Section 6.

2. Construction of SNNs with different topologies

The SNNs with different topologies are constructed, in which network nodes are presented by Izhikevich neuron models, network edges are presented by synaptic plasticity models with time-delay, and network topologies are SW-SFN, SWN, SFN, random network and regular network, respectively.

2.1. Izhikevich neuron model

On account of the advantages in conforming well to firing characteristics of bio-neurons and low computational cost, Izhikevich neuron model is employed as the node in the SNNs, which is described as follows.

$$\begin{aligned} &\tfrac{dv}{dt} = 0.04v^2 + 5v + 140 - u + I_{ext} + I_{syn} \\ &\tfrac{du}{dt} = a(bv - u) \\ &if\ \ v \geq 30,\ \ then \begin{cases} v \leftarrow c \\ u \leftarrow u + d \end{cases} \end{aligned} \tag{1}$$

where v represents the neuronal membrane potential; u represents the resilient variate of v; I_{ext} represents the external input current; I_{syn} represents the total synaptic current; a, b, c, and d are the non-dimensional parameters, different neuronal firing patterns can be obtained by changing their values. In this study, the firing patterns of regular spiking and low-threshold spiking are employed as the firing patterns of excitatory neurons and inhibitory neurons, respectively. And their parameter settings in Izhikevich neuron model are presented in Table 1 [10].

2.2. Synaptic plasticity model with time-delay

The synaptic plasticity model with time-delay is employed as the edge in the SNNs, in which excitatory synapses and inhibitory synapses are included. The model is described as follows.

$$\begin{aligned} &I_{syn} = g_{syn} r (E - V_{post}), \\ &\tfrac{dr}{dt} = \alpha T(1 - r) - \beta r, \\ &T = \tfrac{1}{1 + exp\left(-V_{pre}(t - \tau)\right)} \end{aligned} \tag{2}$$

where I_{syn} represents the total synaptic current; g_{syn} represents the synaptic weight; r represents the receptor binding fraction; V_{pre} and V_{post} represent the membrane potential of the presynaptic neuron and the postsynaptic neuron, respectively; T represents the neurotransmitter concentration; and τ represents the random synaptic time-delay. Considering that the synaptic time-delay in bio-neurons fluctuates randomly within the scope of 0.1–40 ms [20], τ is set to conform to the Poisson distribution covering the scope of synaptic time-delay in bio-neurons. Through changes in g_{syn}, the synaptic plasticity model with time-delay (excitatory and inhibitory synaptic plasticity) regulates the information interaction between presynaptic neurons and postsynaptic neurons. The regulation can be described as follows.

(1) When action potential from the presynaptic neuron i is not transmitted to the postsynaptic neuron j, the excitatory synaptic weight g_{ex} and the inhibitory synaptic weight g_{in} decay exponentially as follows.

$$\begin{aligned} &\mu_{ex} \tfrac{dg_{ex}}{dt} = -g_{ex}, \\ &\mu_{in} \tfrac{dg_{in}}{dt} = -g_{in} \end{aligned} \tag{3}$$

(2) When the action potential from the presynaptic neuron i is transmitted to the postsynaptic neuron j, then g_{ex} and g_{in} are regulated by the spike timing-dependent plasticity rule as follows.

$$\begin{cases} g_{ex}(t) = g_{ex}(t) + \bar{g}_{ex} \\ \bar{g}_{ex} = m_{ij} * g_{max} \end{cases}, \quad m_{ij} = \begin{cases} A_+ \exp(\Delta t / t_+), \Delta t < 0 \\ -A_- \exp(\Delta t / t_-), \Delta t \geqslant 0 \end{cases} \tag{4}$$

$$\begin{cases} g_{in}(t) = g_{in}(t) + \bar{g}_{in} \\ \bar{g}_{in} = n_{ij} * g_{max} \end{cases}, \quad n_{ij} = \begin{cases} -B_+ \exp(\Delta t / t_+), \Delta t < 0 \\ B_- \exp(\Delta t / t_-), \Delta t \geqslant 0 \end{cases} \tag{5}$$

where $\bar{g}_{ex}$ and $\bar{g}_{in}$ represent the increments of g_{ex} and g_{in}, respectively; Δt represents the neuronal firing interval between the presynaptic neuron and postsynaptic neuron; g_{max} represents the maximum value of synaptic weight. If g_{syn} is higher than g_{max}, it is set to g_{max}; If g_{syn} is lower than zero, it is set to zero. In this study,

Table 1
Parameter settings in Izhikevich neuron model.

Parameters	Description	Values
a	Time scale of u	0.02 (excitatory) 0.02 (inhibitory)
b	Sensitivity to v	0.20 (excitatory) 0.25 (inhibitory)
c	Reset value of v	-65 (excitatory) −65 (inhibitory)
d	Reset value of u	8 (excitatory) 2 (inhibitory)

Table 2
Parameter settings in Synaptic plasticity model.

Parameters	Description	Values
E [43]	Synaptic reversible potential	0 mV (excitatory) −70 mV (inhibitory)
α [43]	Forward rate constants	2 (excitatory) 0.9 (inhibitory)
β [43]	Reverse rate constants	1 (excitatory) 0.1 (inhibitory)
τ [20]	Synaptic time-delay	0.1–40 ms
μ_{ex} [44]	Decay constants of g_{ex}	3 ms
μ_{in} [44]	Decay constants of g_{in}	5 ms
g_{max} [44]	Maximum of g_{syn}	0.015
A_+[44]	Maximum correction values of strengthened g_{ex}	0.1
A_-[44]	Maximum correction values of weakened g_{ex}	0.105
B_+[44]	Maximum correction values of strengthened g_{in}	0.02
B_-[44]	Maximum correction values of weakened of g_{in}	0.03
τ_+ [44]	Neuronal firing interval for strengthened g_{syn}	20 ms
τ_-[44]	Neuronal firing interval for weakened g_{syn}	20 ms

the parameter settings in synaptic plasticity model are presented in Table 2.

2.3. Topology generation of SNNs

The topologies of the five SNNs are generated by generation algorithms, and the topological characteristics are further analyzed.

2.3.1. Generation algorithms of topologies

The Barrat-Barthelemy-Vespignani (BBV) algorithm is employed to generate the SW-SFN; the Watts-Strogatz (WS) algorithm is employed to generate the SWN, the regular network, and the random network; the Barabási-Albert (BA) algorithm is employed to generate the SFN.

(1) BBV algorithm

The BBV algorithm [45] can not only simulate the dynamic evolution of the local edge weights caused by adding new nodes but also regulate the ACC within a large scope. Therefore, the BBV algorithm is employed to generate the SW-SFN with both small-world property and scale-free property. The algorithm steps are as follows.

1) A fully connected network including m_0 nodes is generated, in which the initial weights of all edges are assigned as w_0.

2) According to the node-adding probability P_{SWSF}, a new node $n$with m_e edges is added to the network. Each edge of $n$is connected to an existing node in the network based on the weight priority principle:

$$\prod_{n\to i} = \frac{s_i}{\sum_N s_N} s_i = \sum_{j\in\Gamma(i)} w_{ij} \tag{6}$$

where s_i and s_N represent the node intensities of node $i$and all node in the network, respectively; w_{ij} represents the weight between node $i$and its neighbor nodes j.

3) According to the edge-adding probability $1-P_{SWSF}, m_t$ edges are added to the network based on the triad formation mechanism. That is, an edge randomly selected in the network is defined as (x,y). According to the weight priority principle, the neighbor node of $y$excluding $x$is selected and defined as z. If no edge exists between node $x$and node z, a new edge is generated between them; if an edge exists, the weight w_{xz} increases by 1. In both cases, w_{xy} and w_{yz} increase by 1.

By adjusting P_{SWSF} and network parameters, SW-SFNs with different topological characteristics can be generated. In this study, $P_{SWSF}\in(0,1], m_0=5, m_e=3, m_t=2, w_0=1$.

(2) WS algorithm

The WS algorithm [46] integrates the topological advantages of high ACC and low ASPL, which is employed to generate the SWN. The algorithm steps are as follows.

1) A nearest-neighbor coupled network with Nnodes is generated, where each node is connected to its $k$nearest-neighbor nodes and conforms to $\ln N < k < N$.

2) Each edge in the network is randomly reconnected with reconnection probability P_{SW}, that is, for each edge in the network, one endpoint is fixed, and the other endpoint is randomly connected to the other nodes in the network with probability P_{SW}.

By adjusting P_{SW} and network parameters, SWNs with different topological characteristics can be generated. In this study, $P_{SW}\in(0,1), N=500, k=20$. In addition, the generated topology is a regular network at $P_{SW}=0$, the generated topology is a random network at $P_{SW}=1$.

(3) BA algorithm

The BA algorithm [47] can generate an SFN whose degree distribution conforms to power-law distribution. The algorithm steps are as follows.

1) A fully connected network including m_0 nodes is generated.

2) A new node $n$with m_e edges is added to the network. Each edge of $n$is connected to an existing node $i$in the network depends on the node degree k_i.

$$\prod(k_i) = \frac{k_i}{\sum_N k_N} \tag{7}$$

By adjusting network parameters m_0 and m_e, SFNs with different topological characteristics can be generated.

2.3.2. Parameter selection based on topological characteristics

To obtain the optimal network topology generated by each algorithm above, we analyze the generated network based on the topological characteristics including ACC, ASPL, small-world property and scale-free property.

(1) Average clustering coefficient

The ACC reflects the average agglomeration degree of all nodes in a network to present the local information transmission efficiency of the network, which is described as follows.

$$C = \frac{1}{N}\sum_{i=1}^{N}\frac{2e_i}{k_i(k_i-1)} \tag{8}$$

where e_i represents the number of existing edges among the neighbor nodes of node i; k_i represents the degree of node i; N represents the total number of nodes in the network. The larger the C is, the stronger the agglomeration degree of the network is, which means the better the local information transmission efficiency is.

(2) Average shortest path length

The ASPL reflects the average of the shortest distance between all pairs of nodes to present the global information transmission efficiency of a network, which is described as follows.

$$L = \frac{1}{N(N-1)} \sum_{i,j \in V, i \neq j} d_{ij} \tag{9}$$

where d_{ij} represents the shortest distance between node $i$and node j. The smaller the L is, the better the global information transmission efficiency of the network is.

(3) Small-world property

Small-world property σ integrates the topological advantages of high ACC and low ASPL, which is quantitatively described as follows.

$$\sigma = \frac{C_{real}/C_{random}}{L_{real}/L_{random}} \tag{10}$$

where C_{real} and C_{random} represent the ACC of the real network and the corresponding random network with the same nodes number and degree distribution, respectively; L_{real} and L_{random} represent the ASPL of the real network and the corresponding random network with the same nodes number and degree distribution, respectively. When $\sigma > 1$, the network has a small-world property.

(4) Scale-free property

The scale-free property is introduced to describe the heterogeneity of complex systems. The degree distribution of nodes in networks with scale-free property conforms to power-law distribution, and the power-law index γ is within the scope of [2, 3]. The degree distribution of nodes in an SFN is as follows.

$$P(k) \sim k^{-\gamma} \tag{11}$$

In this study, the size of network is 500 nodes. To select the optimal P_{SWSF} of the SW-SFN, we analyze topological characteristics of the SW-SFNs with different P_{SWSF} generated by the BBV algorithm. The results are presented in Table 3.

As can be seen from Table 3, when P_{SWSF} is within the scope of [0.3, 0.9], the γ is within the scope of [2,3], which means that the generated networks have scale-free property. When P_{SWSF} is 0.3, the γ of the generated SW-SFN is 2.165, which most conforms to the results of biological experiment, that is, the γ of the biological functional brain networks is about 2 [33–35]. In addition, σ is 1.8865 when P_{SWSF} is 0.3, which is the largest and conforms to the range of small-world property of biological functional brain network [27,30–32]. Meanwhile, within the P_{SWSF} scope of [0.3, 0.9], the $C$is the highest and the $L$is the lowest when P_{SWSF} is 0.3, which means the highest local and global information transmission efficiency. Therefore, the SW-SFN with $P_{SWSF} = 0.3$ is employed as the topology to construct the CSNN.

To select the optimal P_{SW} of the SWN, we analyze topological characteristics of the SWNs with different P_{SW} generated by the WS algorithm. The results are presented in Table 4.

As can be seen from Table 4, when P_{SW} is 0.6, 0.7, or 0.8, the σ of the generated SWN is 1.8847, 1.4322, and 1.1153, respectively, which conforms to the range of small-world property of biological functional brain network [27,30–32]. Meanwhile, within the P_{SW} scope of [0.6, 0.8], the σ is the highest when P_{SW} is 0.6. In addition, σ of the SWN with $P_{SW} = 0.6$ is basically the same as that of the SW-SFN with $P_{SWSF} = 0.3$. Therefore, the SWN with $P_{SW} = 0.6$ is employed as the topology to construct the SWSNN. For the random SNN and the regular SNN, the network topologies are generated by WS algorithm at $P_{SW} = 1$ and $P_{SW} = 0$, respectively.

To generate an SFN whose power-law index γ conforms to the biological experiment results which is about 2 [33–35], we repeatedly adjust m_0 and m_e. When m_0 is set to 8 and m_e is set to 3, γ of the generated SFN is 2.163, which is basically consistent with γ of the SW-SFN with $P_{SWSF} = 0.3$. Therefore, the SFN with $\gamma = 2.163$ is employed as the topology to construct the SFSNN.

Based on the analysis above, the five kinds of network topologies are set. In order to more clearly present the topology of each generated network, we reduce the node number from 500 to 100 in Fig. 1.

2.4. Construction process of SNNs with different topologies

The construction of the SNNs with different topologies is carried out on a PC with a 4.9 GHz Intel(R) Core i7-9700 k CPU and a 16 GB RAM. The specific construction process is as follows.

(1) According to the generation algorithms presented in Section 2.3.1, we generate five kinds of network topologies, including SW-SFN, SWN, SFN, random network and regular network, in which the size of each network is 500 nodes.
(2) We implement the Izhikevich neuron model according to Eq. (1), and introduce it into the points in the generated networks, in which excitatory neurons and inhibitory neurons are randomly assigned in the ratio of 4:1 based on the results of mammalian cortical neuroanatomy [48].
(3) We implement the synaptic plasticity model with time-delay according to Eqs. (2)–(5)), and introduce it into the edges in the generated networks, in which the synaptic plasticity model is co-regulated by excitatory synapses and inhibitory synapses.

Thus, five kinds of SNNs with different topologies are constructed.

3. Anti-disturbance ability under external noise

To investigate the robustness of the SNNs with different topologies, the anti-disturbance abilities of the CSNN, the SWSNN, the SFSNN, the random SNN, and the regular SNN are comparatively assessed based on two kinds of anti-disturbance indicators under three types of external noise.

3.1. External noise and anti-disturbance indicators

Three types of external noise are introduced as external disturbance, and two anti-disturbance indicators are introduced to assess the anti-disturbance ability of the SNNs with different topologies.

3.1.1. External noise

Electric field noise, white Gaussian noise and impulse noise are introduced as external disturbance, which are common noises

Table 3
Topological characteristics of the SW-SFNs with different P_{SWSF}.

P_{SWSF}	0.1	0.2	**0.3**	0.4	0.5	0.6	0.7	0.8	0.9	1.0
C	0.7028	0.6236	**0.5128**	0.4707	0.4180	0.3884	0.3133	0.2524	0.1889	0.1643
L	2.2836	2.3450	**2.4601**	2.4920	2.5535	2.5627	2.6624	2.7205	2.8354	2.8548
γ	1.551	1.823	**2.165**	2.405	2.513	2.759	2.863	2.872	2.975	3.177
σ	1.3108	1.5256	**1.8865**	1.7338	1.6905	1.6636	1.6327	1.5008	1.4732	1.1260

Table 4
Small-world property of the SWNs with different P_{SW}.

P_{SW}	0.1	0.2	0.3	0.4	0.5	**0.6**	0.7	0.8	0.9
σ	12.2816	9.8966	6.1063	4.6810	3.2293	**1.8847**	1.4322	1.1153	0.9801

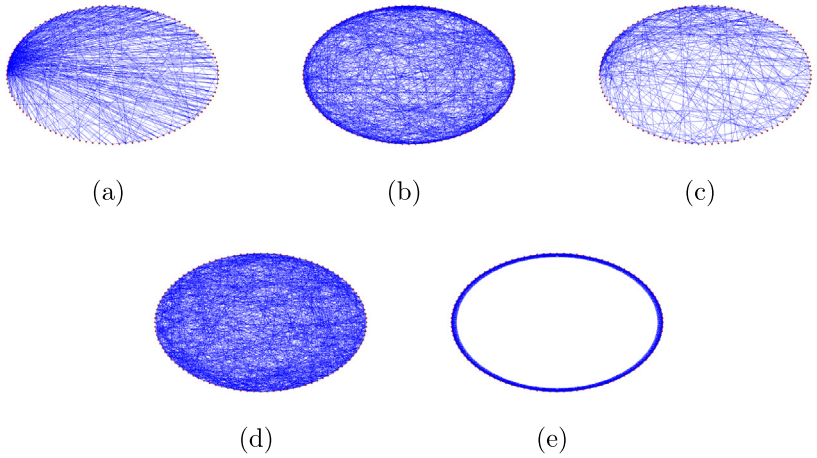

Fig. 1. Topological diagram of the generated networks with 100 nodes. (a) SW-SFN. (b) SWN. (c) SFN. (d) Random network. (e) Regular network.

affecting the function of communication system and electrical equipment.

(1) Electric field noise
The alternating electric field $V(t)$ can be described as follows.

$$V(t) = \psi \frac{A_v}{\omega} sin(\omega t) \tag{12}$$

where ψ represents the length of the polarization; A_v and ω represent the intensity and the angular frequency of the external electric field, respectively. In our simulation, ψ is set to 1 mm; ω is $2\pi f$, in which $f$is electric field frequency. Electric field noise is applied to all neuron models in the SNNs, which is regarded as a voltage disturbance on membrane potential $v$in Eq. (1).

(2) White Gaussian noise
The instantaneous intensity A_g of white Gaussian noise obeys Gaussian distribution, which can be described as follows.

$$f(A_g) = \frac{1}{\sqrt{2\pi}\sigma_g} exp - \frac{\left(A_g - \mu_g\right)^2}{2\sigma_g^2} \tag{13}$$

where μ_g represents the average of A_g; σ_g represents the standard deviation of A_g. In our simulation, white Gaussian noise is applied to all neuron models in the SNNs, which is regarded as a current disturbance on the external input current I_{ext} in Eq. (1).

(3) Impulse noise
Impulse noise is composed of irregular discontinuous impulse spikes, which is characterized by short duration, large amplitude and burst. Its mathematical description can be described as follows.

$$s(t) = \begin{cases} A_s, t \in [T_0, T_0 + T_s] \\ 0, else \end{cases} \tag{14}$$

where A_s represents the impulse intensity; T_0 represents the start time of stimulation; T_s represents the duration of stimulation. In our simulation, T_s is set to 200 ms. Impulse noise is applied to all neuron models in the SNNs, which is regarded as a current disturbance on the external input current I_{ext} in Eq. (1).

The electric field noise, white Gaussian noise and impulse noise are shown in Fig. 2.

3.1.2. Anti-disturbance indicators

We assess the anti-disturbance ability of the SNNs using two anti-disturbance indicators including the relative change in firing rate and the correlation between membrane potential.

(1) The relative change in firing rate
The firing rate of a neuron represents the frequency of neuronal firing per unit time. The relative change in firing rate δ can characterize the change degree of neuronal firing rate of an SNN before and after noise disturbance, which is described as follows.

$$\delta = \frac{1}{N} \sum_{i=1}^{N} \left(\frac{|f_{ia} - f_{ib}|}{f_{ib}} \right) * 100\% \tag{15}$$

where f_{ib} and f_{ia} represent the neuronal firing rate of a single neuron before and after noise disturbance, respectively. The smaller the δ is, the better the anti-disturbance ability of the SNN is.

(2) The correlation between membrane potential
The correlation between membrane potential ρ can characterize the similarity between neuronal membrane potential of an SNN before and after noise disturbance, which is described as follows.

$$\rho = \frac{1}{N} \sum_{i=1}^{N} \left(\frac{\sum_{t=t_1}^{t_2-\Delta t+1} x_{ib}(t) x_{ia}(t+\Delta t)}{\sqrt{\sum_{t=t_1}^{t_2-\Delta t+1} x_{ib}^2(t) \sum_{t=t_1}^{t_2-\Delta t+1} x_{ia}^2(t+\Delta t)}} \right) \tag{16}$$

where x_{ib} and x_{ia} represent the membrane potential of a single neuron before and after noise disturbance, respectively; $[t_1, t_2]$ represents the simulation duration. The larger the ρ is, the better the anti-disturbance ability of the SNN is.

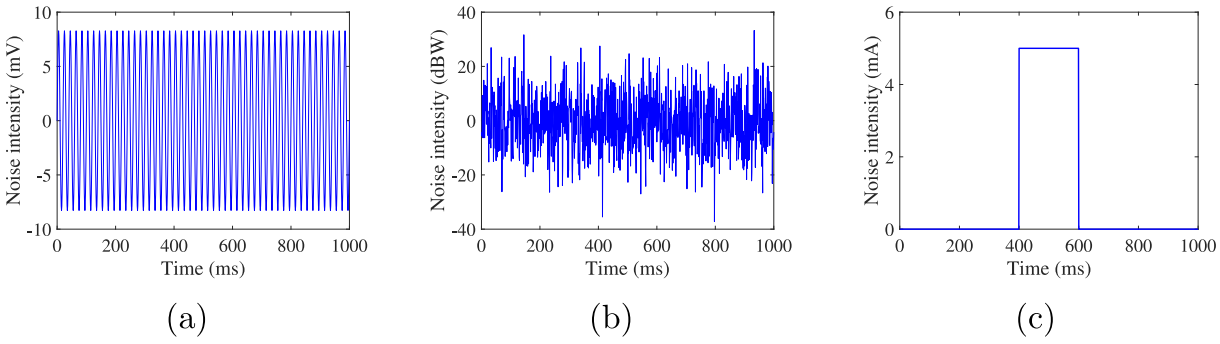

Fig. 2. The three kinds of noise. (a) Electric field noise. (b) White Gaussian noise. (c) Impulse noise.

3.2. Anti-disturbance comparison of SNNs with different topologies

To investigate the effect of network topologies on the robustness of SNNs, we comparatively assess the anti-disturbance abilities of the CSNN, the SWSNN, the SFSNN, the random SNN, and the regular SNN based on δ and ρ under electric field noise, white Gaussian noise and impulse noise, respectively.

We first investigate the effect of network topologies on anti-disturbance abilities of the SNNs under different intensity of external noise. The scopes of noise intensity are as follows: the intensity of electric field noise with the frequency of 50 Hz is within the scope of [0, 48] mV with the step length of 6 mV; the white Gaussian noise intensity is within the scope of [0, 24] dBW with the step length of 3 dBW; the intensity of impulse noise is within the scope of [0, 8] mA with the step length of 1 mA. The anti-disturbance abilities of the five SNNs based on δ under different intensity of external noise are shown in Fig. 3, and the anti-disturbance abilities of the five SNNs based on ρ under different intensity of external noise are shown in Fig. 4.

For electric field noise, white Gaussian noise and impulse noise, we can draw the same conclusions from Fig. 3 as follows. (i) In terms of noise intensity, δ of the five SNNs progressively increases with the increasement of noise intensity. (ii) In terms of different network topologies, δ of the CSNN is lower than that of the SWSNN, δ of the SWSNN is lower than that of the SFSNN, δ of the SFSNN is lower than that of the random SNN and regular SNN, and δ of the random SNN and regular SNN are similar.

For electric field noise, white Gaussian noise and impulse noise, we can draw the same conclusions from Fig. 4 as follows. (i) In terms of noise intensity, ρ of the five SNNs progressively decreases with the increasement of noise intensity. (ii) In terms of different network topologies, ρ of the CSNN is higher than that of the SWSNN, ρ of the SWSNN is higher than that of the SFSNN, ρ of the SFSNN is higher than that of the random SNN and regular SNN, and ρ of the random SNN and regular SNN are similar.

In addition, we further investigate the effect of network topologies on anti-disturbance abilities of the SNNs under different frequency of external noise. For white Gaussian noise, its instantaneous intensity obeys Gaussian distribution, and its power spectral density is constant over the whole frequency range. For impulse noise, a single impulse disturbance is performed during the simulation duration since the interval of impulse noise is usually larger than 1 s. Therefore, we only investigate the anti-disturbance ability of the five SNNs based on δ and ρ under different frequency of electric field noise. The electric field noise with intensity of 24 mV is taken as an example, and the frequency is within the scope of [0, 100] Hz with the step length of 10 Hz. The anti-disturbance abilities of the five SNNs under different frequency of electric field noise are shown in the Fig. 5.

From Fig. 5, we can draw the conclusions as follows. (i) In terms of noise frequency, with the increasement of electric field frequency, δ of the five SNNs progressively increases, and ρ of the five SNNs progressively decreases. (ii) In terms of different network topologies, δ of the CSNN is lower than that of the SWSNN, δ of the SWSNN is lower than that of the SFSNN, δ of the SFSNN is lower than that of the random SNN and regular SNN, and δ of the random SNN and regular SNN are similar; ρ of the CSNN is higher than that of the SWSNN, ρ of the SWSNN is higher than that of the SFSNN, ρ of the SFSNN is higher than that of the random SNN and regular SNN, and ρ of the random SNN and regular SNN are similar.

In summary, based on δ and ρ under electric field noise, white Gaussian noise and impulse noise, our simulation consistently certifies that: (i) The five SNNs with different topologies have anti-disturbance ability, and the anti-disturbance ability decreases with the increasement of noise intensity and/or frequency. (ii) Network topologies affect anti-disturbance ability of the SNNs. In terms of

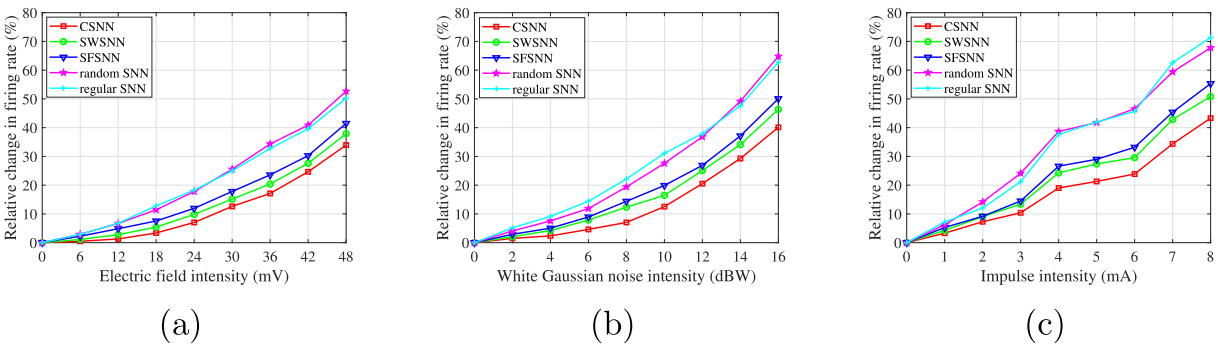

Fig. 3. Anti-disturbance comparison based on δ under different intensity of external noise. (a) Electric field noise. (b) White Gaussian noise. (c) Impulse noise.

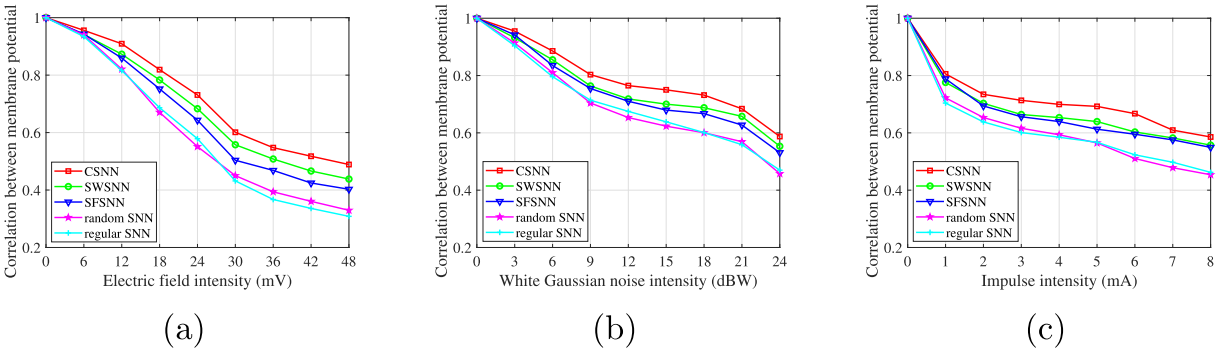

Fig. 4. Anti-disturbance comparison based on ρ under different intensity of external noise. (a) Electric field noise. (b) White Gaussian noise. (c) Impulse noise.

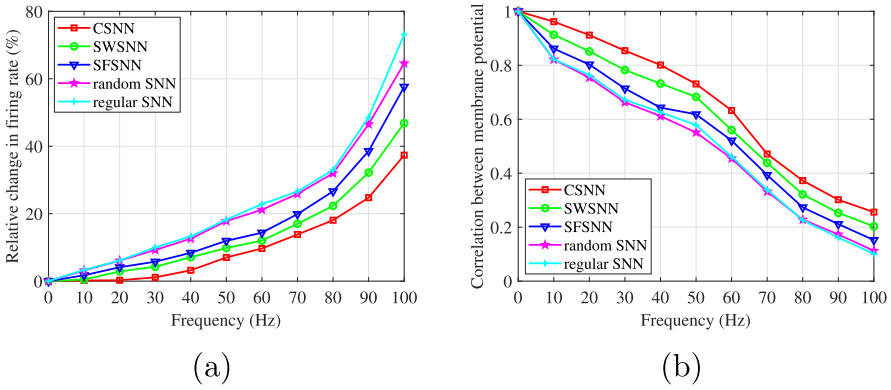

Fig. 5. Anti-disturbance comparison based on δ and ρ under different frequency of electric field noise. (a) δ. (b) ρ.

anti-disturbance performance, the CSNN outperforms the SWSNN, the SWSNN outperforms the SFSNN, the SFSNN outperforms the random SNN and regular SNN, and the random SNN and regular SNN are tied. These results indicate that network topologies affect anti-disturbance ability of the SNNs, which hints that SNNs with more biological rationality have better robustness.

3.3. Significance test for anti-disturbance ability

To verify the significant statistical difference between the anti-disturbance ability of the five kinds of SNNs, Friedman test is introduced to conduct significance test on δ and ρ of the SNNs under different noise. The mathematical description is as follows.

$$F_f = \frac{12n_t}{k_t(k_t+1)}\left[\sum_{i=1}^{k} R_i^2 - \frac{k_t(k_t+1)^2}{4}\right] \tag{17}$$

where Rrepresents the average rank; k_t represents the number of tested objects; n_t represents the data length of each object. In this study, Rrepresents the average rank of anti-disturbance ability of each SNN; k_t represents the number of SNNs with different topologies; n_t represents the data length of the anti-disturbance indicators. The F_f is compared with the F_α at the significance level 0.05 (i.e. $\alpha = 0.05$). F_α is 2.714 by searching the critical values table of Friedman test. If $F_f > F_\alpha$, there is significant statistical difference between the anti-disturbance ability of the five kinds of SNNs. The results of Friedman test on δ and ρ of the five kinds of SNNs under electric field noise, white Gaussian noise, and impulse noise are shown in Table 5.

Table 5
Results of Friedman test on δ and ρ.

F_f	Types of external noise		
	Electric field noise	White Gaussian noise	Impulse noise
δ	31.2	30.8	30.4
ρ	30.6	29.8	29.7

As can be seen from Table 5, the values of all F_f are invariably higher than the value of F_α, which means that the significant statistical difference exists in the anti-disturbance ability of SNNs with different topologies under electric field noise, white Gaussian noise or impulse noise. Further, the two-tailed Nemenyi test is introduced to quantitatively characterize the difference of anti-disturbance ability, the critical difference of which is described as follows.

$$CD = q_{0.05}\sqrt{\frac{k_t(k_t+1)}{6n_t}} \tag{18}$$

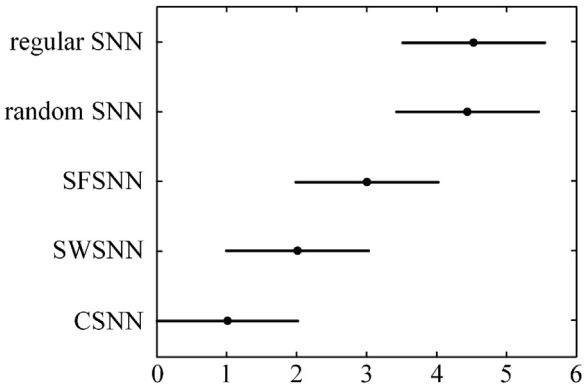

Fig. 6. Results of the two-tailed Nemenyi test.

where k_t represents the number of SNNs with different topologies; n_t represents the data length of the anti-disturbance indicators; $q_{0.05}$ is 2.728 by searching the critical values table. Thus, *CD*is 2.157 in this study. The results of the two-tailed Nemenyi test are shown in Fig. 6.

In Fig. 6, the dot represents the average rank of each SNN, and the black bar represents the *CD*. Fig. 6 presents the average rank of each SNN, that is, the order in anti-disturbance ability of the five kinds of SNNs with different topologies. In terms of anti-disturbance performance, the CSNN, the SWSNN, and the SFSNN have significant statistical difference, and the random SNN and the regular SNN are ranked in a similar order, which is consistent with the conclusion in Section 3.2.

In summary, the results of significance test verify the validity of our conclusion about the anti-disturbance ability of the five kinds of SNNs with different topologies from the perspective of statistics.

4. Case study of speech recognition task under disturbance

On the basis of the results of anti-disturbance ability above, the speech recognition task is taken as a case study to further certify the anti-disturbance ability of the SNNs with different topologies in application, in which the recognition accuracy is introduced to assess the performance of the SNNs. The speech recognition dataset is a subset in the TI 46-Word of isolated digits from the speech database of the Linguistic Data Consortium (https://catalog.ldc.upenn.edu/LDC93S9), which includes read utterances of the digits "zero" through "nine" from eight females and eight males English speakers.

4.1. Speech recognition framework based on the SNNs

Learning from the Liquid State Machine (LSM) framework, we design a speech recognition framework based on our SNNs, including input layer, reserve layer, and output layer, which is shown in Fig. 7.

According to Fig. 7, the process of speech recognition is presented as follows.

(1) The input layer includes 77 Izhikevich neuron models to receive the speech spike trains, which are preprocessed by Lyon ear model and Bens Spiker Algorithm (BSA). Lyon ear model converts the continuous temporal speech waveform into analog signal of 77 frequency bands [49]. Then, these analog signals are encoded into 77 spike trains based on the BSA so that Izhikevich neuron models in input layer can receive [50].
(2) The reserve layer is our SNN with anti-disturbance ability above. The input layer transmits spike trains of speech signal into the Izhikevich neuron models of the SNN in reserve layer, which induces a series of firing activities of the neurons in the SNN. The induced nonlinear dynamic behavior can project the low-dimensional spike train into a high-dimensional feature space where the different patterns are easier to be computed and separated.
(3) The output layer includes 10 Izhikevich neuron models. The synaptic weights between reserve layer and output layer are trained by a Remote Supervised Method (ReSuMe) [51], which is a supervised learning algorithm with biological rationality since the process of training synaptic weights obeys the Hebbian rule. The ReSuMe algorithm is carried out according to the desired output template set by each digital speech, which regulates the firing activity of Izhikevich neuron models in output layer to obtain the speech recognition results.

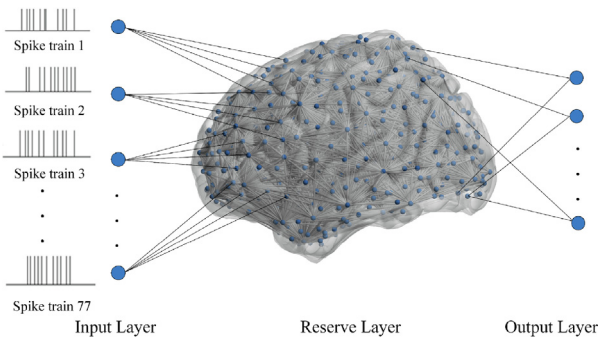

Fig. 7. Speech recognition framework based on the SNN.

4.2. Speech recognition results

To further certify the anti-disturbance ability in application, the speech recognition accuracies of the five SNNs under three types of external noise are compared with that of the five SNNs without disturbance, respectively. The electric field noise with the intensity of 24 mV and the frequency of 50 Hz, the white Gaussian noise with the intensity of 12 dBW, and the impulse noise with the intensity of 4 mA are taken as the examples, respectively. The speech recognition dataset is randomly divided into a training set and a test set, which contains 2400 utterances in training set (10 digits $\times$ 16 speakers $\times$ 15 utterances) and 1600 utterances in test set (10 digits $\times$ 16 speakers $\times$ 10 utterances). The results of speech recognition accuracy in test set are shown in Table 6.

From Table 6, it can be seen that: (1) No matter with or without disturbance, the recognition accuracy of the CSNN outperforms that of the SWSNN and the SFSNN, and all of them outperform the random SNN and the regular SNN, which is consistent with the order of anti-disturbance ability based on δ and ρ above. The results verify the effectiveness of anti-disturbance indicators (δ and ρ) to assess the anti-disturbance ability of SNNs. (2) Compared with the five kinds of SNNs without disturbance, these SNNs can remain almost the same recognition accuracy under the three types of external noise. And the difference in recognition accuracy of CSNN is less than that of other SNNs. Therefore, results of speech recognition performance certify that the CSNN with more biological rationality has better anti-disturbance ability, which hints that SNNs with more biological rationality have better robustness.

5. Discussion

From Section 3 and Section 4, our results consistently certify the anti-disturbance ability of the five SNNs under different external noise from the changes in firing activities (δ and ρ) in brain-like models and the application in speech recognition of brain-like models, and the CSNN with both small-world property and scale-free property has the best anti-disturbance ability in them. On this basis, the anti-disturbance mechanism is further discussed based on the evolution processes of neural information in the CSNN under three types of external noise. The electric field noise with the intensity of 24 mV and the frequency of 50 Hz, the white Gaussian noise with the intensity of 12 dBW, and the impulse noise with the intensity of 4 mA are taken as the examples, respectively.

5.1. Firing rate

To investigate the changes in neuronal firing patterns under external noise, we present the firing sequences of the single Izhikevich neuron model with and without external noise, which are shown in Fig. 8.

Table 6
Speech recognition accuracies of SNNs under disturbance.

Recognition accuracies	SNNs with different topologies				
	CSNN	SWSNN	SFSNN	random SNN	regular SNN
Electric field noise	93.01%	91.85%	90.45%	86.03%	86.11%
White Gaussian noise	93.04%	91.82%	90.52%	86.12%	86.06%
Impulse noise	92.95%	91.79%	90.41%	85.86%	85.56%
Without disturbance	93.21%	92.30%	91.26%	87.89%	87.33%

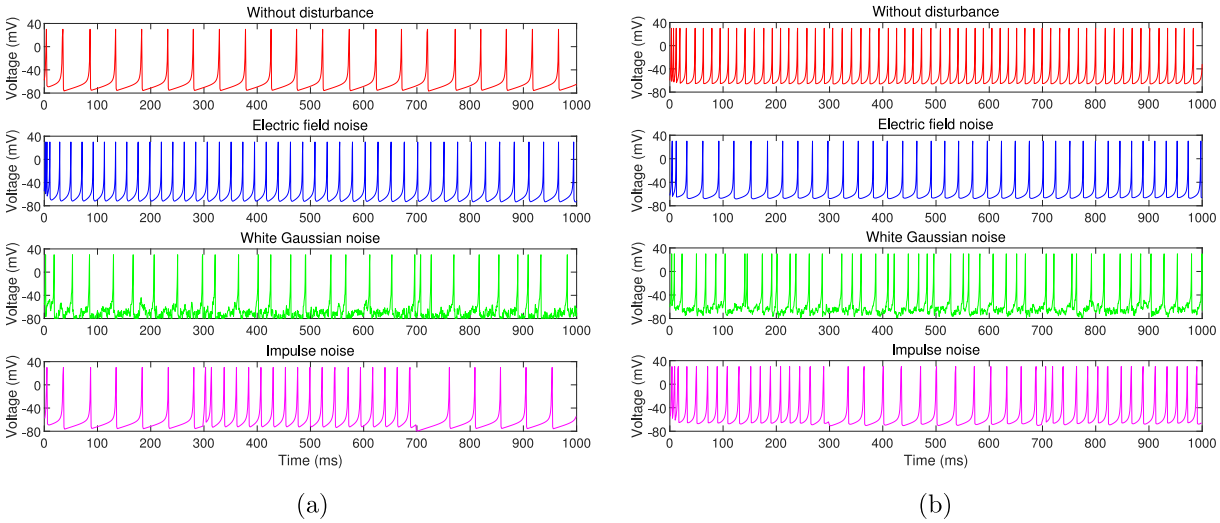

Fig. 8. Firing sequences of single Izhikevich neuron model. (a) Excitatory neuron. (b) Inhibitory neuron.

From Fig. 8, the firing sequences of excitatory and inhibitory Izhikevich neuron models change obviously under external noise, compared with that of the neuron models without disturbance. It indicates that external noise can affect the neuronal firing patterns. The average firing rate in the CSNN is characterized by the average of firing rate of all neurons during a time window of 100 ms. The evolution processes of average firing rate in the CSNN under three types of external noise are shown in Fig. 9.

From Fig. 9, the three evolution processes of average firing rate in the CSNN under different external noise present similar trend. In the first 300 ms under external noise, the average firing rate in the CSNN decreases sharply; whereafter, the average firing rate decreases tardily and progressively stabilizes. The explanation for this phenomenon is that: in the initial phase of stimulation, external noise mightily affects the neuronal firing patterns; after a period of self-adaptive regulation of the SNNs, the neuronal firing patterns progressively tends to be stable.

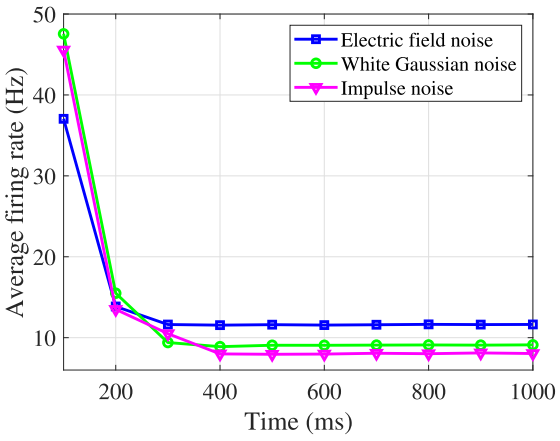

Fig. 9. Evolution processes of average firing rate in the CSNN under external noise.

5.2. Synaptic weight

According to Eqs. (4) and (5), changes in synaptic weight rely on the firing interval between the presynaptic neurons and postsynaptic neurons. Therefore, changes in neuronal firing patterns can induce changes in synaptic weight. The average synaptic weight is the average of the weights of all synapses in an SNN. The sum synaptic weight is the sum of absolute value of all synaptic weights in an SNN. The evolution processes of the average synaptic weight and the sum synaptic weight in the CSNN under three types of external noise are shown in Fig. 10.

From Fig. 10, the three evolution processes of both the average synaptic weight and the sum synaptic weight in the CSNN under different external noise present similar trend. In the first 300 ms under external noise, both the average synaptic weight and the sum synaptic weight in the CSNN decrease sharply; whereafter, they decrease tardily and progressively stabilize. Fig. 10 reflects the self-adaptive changes of synaptic plasticity under external noise.

5.3. Correlation between synaptic plasticity and anti-disturbance ability

To explore the reason of anti-disturbance ability, we first compare the anti-disturbance ability of the CSNN with or without synaptic plasticity under different external noise based on δ and ρ. The results are shown in Fig. 11 and Fig. 12.

From Fig. 11, δ of the CSNN without synaptic plasticity under three types of external noise is significantly higher than that of

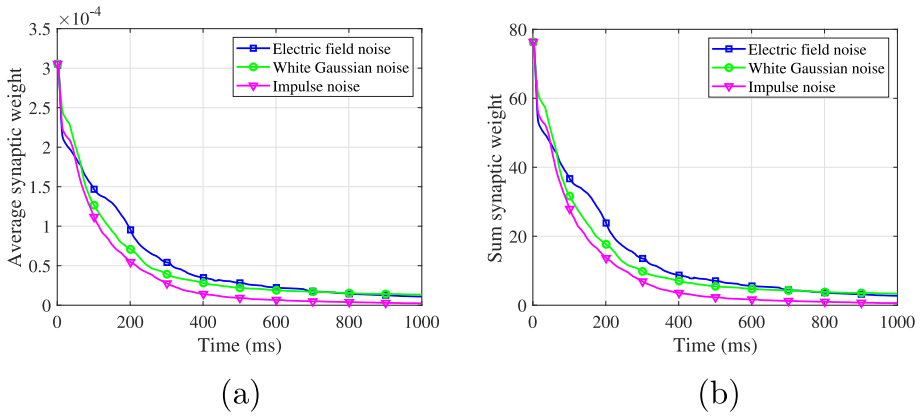

Fig. 10. Evolution processes of synaptic weight in the CSNN under external noise. (a) Average synaptic weight. (b) Sum synaptic weight.

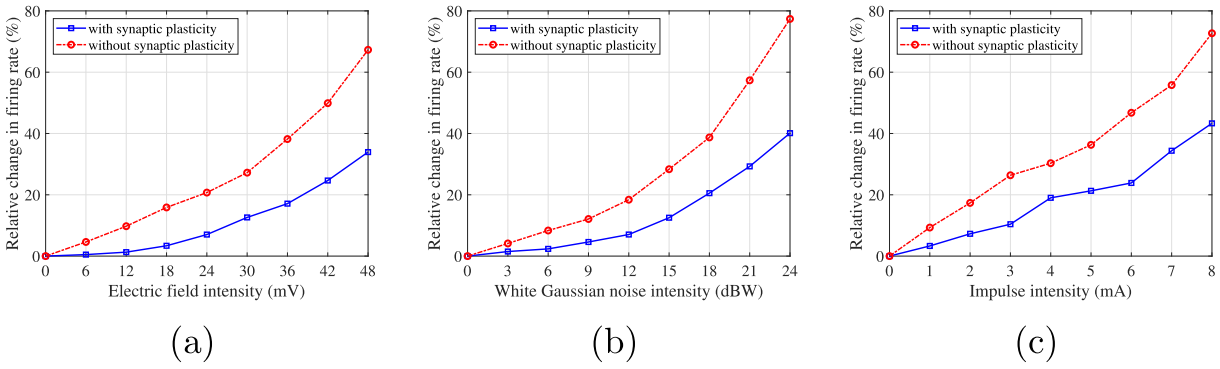

Fig. 11. Anti-disturbance ability of the CSNN with or without synaptic plasticity based on δ. (a) Electric field noise. (b) White Gaussian noise. (c) Impulse noise.

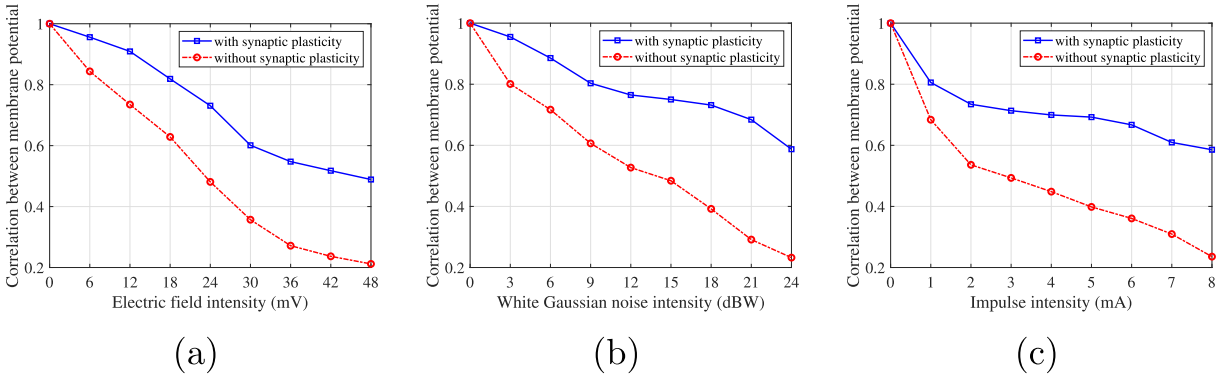

Fig. 12. Anti-disturbance ability of the CSNN with or without synaptic plasticity based on ρ. (a) Electric field noise. (b) White Gaussian noise. (c) Impulse noise.

the CSNN with synaptic plasticity; from Fig. 12, ρ of the CSNN without synaptic plasticity under three types of external noise is significantly lower than that of the CSNN with synaptic plasticity. Therefore, compared with the CSNN with synaptic plasticity, the anti-disturbance ability of the CSNN without synaptic plasticity drastically reduced, which indicates that synaptic plasticity has significant effect on the anti-disturbance ability of the SNNs.

Further, to explore the relationship between the self-adaptive regulation of synaptic plasticity and the anti-disturbance ability of the CSNN with synaptic plasticity, we carry out a Pearson correlation analysis between the average synaptic weight and the anti-disturbance indicators under different external noise. Pearson correlation coefficient r_{XY} can characterize the statistical correlation between sample $X$and sample Y, which is described as follows.

$$r_{XY} = \frac{\sum_{i=1}^{n}(X_i - \overline{X})(Y_i - \overline{Y})}{\sqrt{\sum_{i=1}^{n}(X_i - \overline{X})^2}\sqrt{\sum_{i=1}^{n}(Y_i - \overline{Y})^2}} \tag{19}$$

The closer the absolute value of r_{XY} approaches to 1, the larger the correlation degree between the two samples X and $Y$is. A statistical t-test is carried out to investigate the significance of a sample $r$to the totality, which is defined as follows.

$$t_{test} = \frac{r}{\sqrt{(1-r^2)/(n-2)}} \tag{20}$$

In the results of t-test, "**" means the significant level of 0.01, and "*" means the significant level of 0.05. In this study, Xrepresents the average synaptic weight in the CSNN during a time window of 100 ms; Yrepresents the two anti-disturbance indicators in

the CSNN during a time window of 100 ms; *n*represents the sample size, which is set to 10. The statistical correlation between average synaptic weight and anti-disturbance indicators (δ and ρ) in the CSNN within 1000 ms are shown in Table 7.

From Table 7, under three types of external noise, significant statistical correlation exists between the average synaptic weight and the anti-disturbance indicators at the significant level of 0.01.

In summary, through the comparison of anti-disturbance ability with or without synaptic plasticity and the analysis of Pearson correlation, these results hint that the self-adaptive regulation of synaptic plasticity is the intrinsic factor of anti-disturbance ability of an SNN.

5.4. Effect of network topologies on anti-disturbance ability

To analyze the effect of network topologies on the anti-disturbance ability, we present the evolution processes of weighted ACC and weighted ASPL in SNNs with different topologies under different external noise. The weighted ACC represents the average agglomeration degree of all nodes in an SNN, which can reflect the local information transmission efficiency [52]. Its mathematical description is as follows.

$$\tilde{C_w} = \frac{1}{s_i(k_i-1)N}\sum_{j,k}\frac{(w_{ij}+w_{ik})}{2}a_{ij}a_{jk}a_{ki} \tag{21}$$

where $\tilde{C_w}$ represents the weighted ACC; s_i represents the node strength; k_i represents the node degree; w_{ij} and w_{ik} represent the synaptic weights; a_{ij}, a_{jk}, and a_{ki} represent the adjacent matrices.

The weighted ASPL represents the average of the shortest distance between all pairs of nodes in an SNN, which can reflect global information transmission efficiency [53]. Its mathematical description is as follows.

$$\tilde{L_w} = \frac{1}{N(N-1)}\min_{\Upsilon(i,j)\in\Gamma(i,j)}\left[\sum_{m,n\in\Upsilon(i,j)}\frac{1}{w_{mn}}\right] \tag{22}$$

where $\tilde{L_w}$ represents the weighted ASPL; w_{mn} represents the synaptic weights.

According to Eqs. (21) and (22), changes in synaptic weight can induce changes in $\tilde{C_w}$ and $\tilde{L_w}$. The evolution processes of the weighted ACC and the weighted ASPL in SNNs with non-complex network topologies (random SNN and the regular SNN) and complex network topologies (the CSNN, the SWSNN, and the SFSNN) within 1000 ms under different external noise are shown in Fig. 13 and Fig. 14, respectively.

We unscramble the evolution processes in Fig. 13 and Fig. 14 from the following two aspects.

(1) For the same SNN under different external noise: the evolution processes of weighted ACC present similar trend and level in Fig. 13; the evolution processes of weighted ASPL present similar trend and level in Fig. 14. These results indicate that the evolution processes of topological characteristics in the same SNN under different external noise are similar.

(2) For different SNNs under the same external noise: we analyze the evolution processes of the weighted ACC and the weighted ASPL in SNNs with non-complex network topologies and complex network topologies under different external noise. For electric field noise, white Gaussian noise and impulse noise, we can draw the same conclusions as follows.

1) We analyze the weighted ACC and weighted ASPL in the SNNs with non-complex network topologies. For the random SNN, both weighted ACC and weighted ASPL of the network are the lowest, which means that this kind of SNN has high global information transmission efficiency, but low local information transmission efficiency. For the regular SNN, both weighted ACC and weighted ASPL of the network are the highest, which means that this kind of SNN has high local information transmission efficiency, but low global information transmission efficiency. These analysis results indicate that the local and global information transmission efficiency cannot be integrated in random SNN and regular SNN, which supports the phenomenon that these two SNNs are weak and tied in terms of anti-disturbance performance.
2) We analyze the weighted ACC and weighted ASPL in the SNNs with complex network topologies. For the CSNN, the SWSNN, and the SFSNN, the weighted ACC is in a relatively high level and the weighted ASPL is in a relatively low level, that is, these three SNNs can integrate the local and global information transmission efficiency. These analysis results support the phenomenon that the SNNs with complex network topologies outperform the SNNs with non-complex network topologies in terms of anti-disturbance performance.
3) Among the three kinds of SNNs with complex network topologies, the CSNN has the highest weighted ACC, followed by the SWSNN, and then the SFSNN; the CSNN has the lowest weighted ASPL, followed by the SWSNN, and then the SFSNN. These analysis results indicate that the CSNN, the SWSNN and the SFSNN decrease in turn in both local and global information transmission efficiency, which supports the phenomenon that the CSNN outperforms the SWSNN, the SWSNN outperforms the SFSNN in terms of anti-disturbance performance.

In addition, we deeply discuss the effect of network topologies on the anti-disturbance ability of the SNNs with complex network topologies based on the degree distribution, which can reflect the importance of nodes in SNNs. The results are shown in Fig. 15.

From Fig. 15(a), degree distribution of the SWSNN is bell-shaped and the node degree is relatively concentrated, which means that nodes in the SWSNN are of similar importance and there is no hub node. From Fig. 15(b), degree distribution of the SFSNN conforms to power-law distribution, which means that a few nodes are hub nodes with higher importance, whereas, the majority of nodes are non-hub nodes with trivial importance. The SFSNN has a strong fault tolerance due to the extremely heterogeneous in degree distribution, which supports the anti-disturbance ability of the SFSNN. However, all the nodes are disturbed by external noise in this study, which makes that the anti-disturbance ability of the SFSNN decreases since the hub nodes are involved in. Therefore, these analysis results support the phenomenon that the SWSNN has better anti-disturbance performance than that of the SFSNN.

From Fig. 15(c), degree distribution of the CSNN conforms to power-law distribution, which seems similar to degree distribution of the SFSNN in Fig. 15(b). In depth, compared with the SFSNN, the degree distribution of the CSNN is more decentralized and the degree of hub nodes is larger. The more decentralized degree dis-

Table 7
Statistical correlation between the average synaptic weight and the anti-disturbance indicators.

Statistical correlation	Types of external noise		
	Electric field noise	White Gaussian noise	Impulse noise
δ	−0.915**	−0.897**	−0.885**
ρ	−0.977**	−0.952**	−0.946**

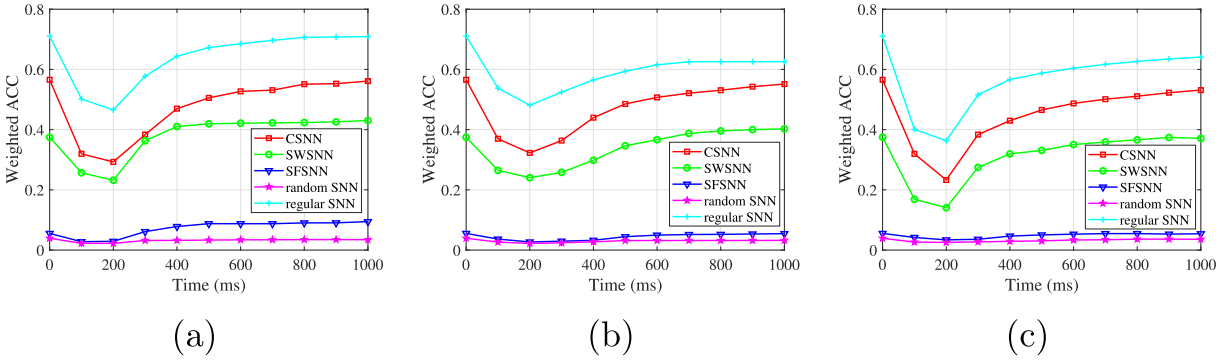

Fig. 13. Evolution processes of the weighted ACC under different external noise. (a) Electric field noise. (b) White Gaussian noise. (c) Impulse noise.

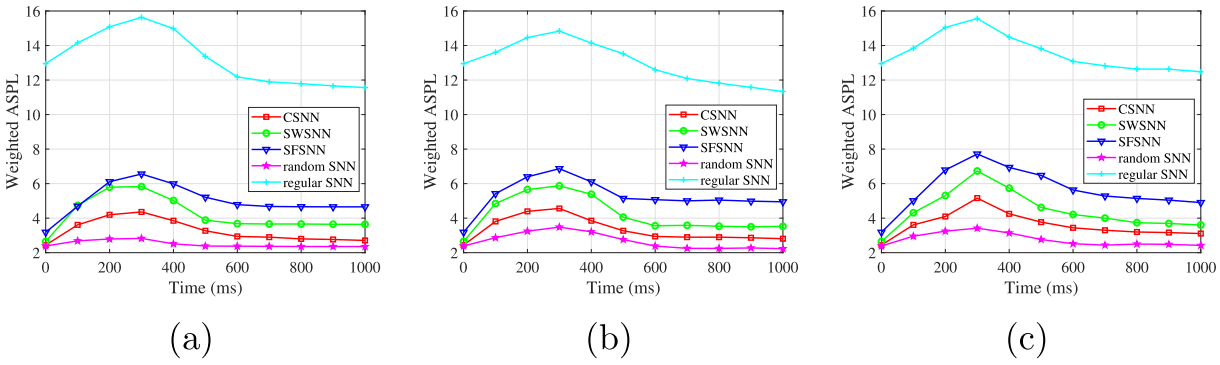

Fig. 14. Evolution processes of the weighted ASPL under different external noise. (a) Electric field noise. (b) White Gaussian noise. (c) Impulse noise.

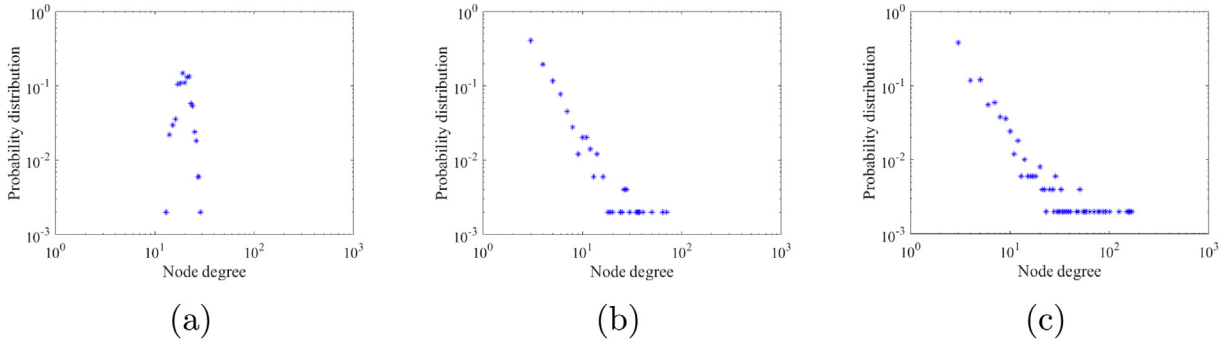

Fig. 15. Degree distribution of complex network topology. (a) SWSNN. (b) SFSNN. (c) CSNN.

tribution makes the synaptic weight (w_{ij} and w_{ik} in Eq. (21)) among the neighbor nodes of the hub node in the CSNN larger, which further results in higher weighted ACC. The larger degree of hub nodes means the larger synaptic weight (w_{mn} in Eq. (22)) connected to the hub nodes in the CSNN, which results in lower weighted ASPL. The higher weighted ACC and lower weighted ASPL make the CSNN has small-world property, which means the CSNN combine the topological advantages of the SWSNN and the SFSNN. Therefore, these analysis results support the phenomenon that the CSNN has better anti-disturbance performance than the SWSNN and the SFSNN.

In summary, different network topologies affect the information transmission efficiency and the degree distribution of nodes in an SNN, which further affects the anti-disturbance performance of the SNN. Our analysis results hint that the network topology is a factor that affects the anti-disturbance ability of SNNs at the level of performance.

6. Conclusion

In this study, the five kinds of SNNs with different topologies are constructed, in which the network nodes are presented by Izhikevich neuron models, the network edges are presented by synaptic plasticity models with time-delay including excitatory and inhibitory synapses, and the network topologies are the SW-SFN, the SWN, the SFN, the random network and the regular network, respectively. Then, the robustness of the SNNs with different topologies is comparatively assessed based on the anti-disturbance ability under different noise. Further, by taking a speech recognition task as the case study, we investigate the anti-disturbance ability of the SNNs in application. Finally, the anti-disturbance mechanism is discussed based on the evolution process of neural information. Our simulation consistently certifies that: (i) The five kinds of SNNs with different topologies have anti-disturbance ability, and the anti-disturbance ability decreases with the increase-

ment of noise intensity and/or frequency. In terms of anti-disturbance performance, the CSNN outperforms the SWSNN, the SWSNN outperforms the SFSNN, all of them outperform the random SNN and the regular SNN, and the random SNN and the regular SNN are tied. The simulation results indicate that SNNs with more biological rationality have better robustness. (ii) In terms of speech recognition performance, the recognition accuracy of the CSNN outperforms that of the SWSNN and SFSNN, and all of them outperform the random SNN and the regular SNN, which is consistent with the order of anti-disturbance ability above. In addition, compared with the five kinds of SNNs without disturbance, these SNNs can remain almost the same recognition accuracy under the three types of external noise. These results verify the effectiveness of anti-disturbance indicators (δ and ρ) to assess the anti-disturbance ability of SNNs. (iii) Through the comparison of anti-disturbance ability with or without synaptic plasticity and the analysis of Pearson correlation, these results hint that the self-adaptive regulation of synaptic plasticity is the intrinsic factor of anti-disturbance ability of an SNN. (iv) The results of evolution processes of topological characteristics including weighted ACC, weighted ASPL and degree distribution hint that the network topology is a factor that affects the anti-disturbance ability at the level of performance. Our simulation results certify that SNNs with more biological rationality have better robustness, which are conducive to the design of neuromorphic chips with robustness at algorithm level. Neuromorphic chips include digital circuits and analog circuits. External noise could affect the function of analog or mixed-signal neuromorphic chips since the computation of neurons and synapses are analog. Therefore, our simulation results could provide a foundation support for the development of neuromorphic algorithms with robustness on analog or mixed-signal neuromorphic chips under complex noise environment. In addition, different neuron models also affect the performance of brain-like models. In our future work, we will further investigate the effect of different neuron models on anti-disturbance ability of the CSNN under external noise, and certify its anti-disturbance ability in applications.

CRediT authorship contribution statement

Lei Guo: Conceptualization, Methodology, Writing – review & editing. **Dongzhao Liu:** Methodology, Formal analysis, Investigation, Writing – original draft. **Youxi Wu:** Writing – review & editing. **Guizhi Xu:** Supervision.

Declaration of Competing Interest

The authors declare that they have no known competing financial interests or personal relationships that could have appeared to influence the work reported in this paper.

Acknowledgements

This work was supported by the National Natural Science Foundation of China (Nos. 52077056, 61976240, 51977060); the Natural Science Foundation of Hebei Province (No. E2020202033); and the Postgraduate Innovation Foundation of Hebei province (No. CXZZBS2021025).

References

[1] C.H. Luo, F.L. Li, P.Y. Li, C.L. Yi, C.B. Li, Q. Tao, X.B. Zhang, Y.J. Si, D.Z. Yao, G. Yin, A survey of brain network analysis by electroencephalographic signals, Cogn. Neurodyn. 16 (1) (2021) 17–41, https://doi.org/10.1007/s11571-021-09689-8.
[2] R. Wang, Y.C. Fan, Y. Wu, Spontaneous electromagnetic induction promotes the formation of economical neuronal network structure via self-organization process, Scientific Rep. 9 (2020) 9698, https://doi.org/10.1038/s41598-019-46104-z.
[3] Q.H. Hong, H.G. Chen, J.R. Sun, C.H. Wang, Memristive circuit implementation of a self-repairing network based on biological astrocytes in robot application, IEEE Trans. Neural Networks Learn. Syst. 99 (2021) 1–15, https://doi.org/10.1109/TNNLS.2020.3041624.
[4] J.B. Wu, Q. Liu, M.L. Zhang, Z.H. Pan, H.Z. Li, K.C. Tan, Hurai: A brain-inspired computational model for human-robot auditory interface, Neurocomputing 465 (2021) 103–113, https://doi.org/10.1016/j.neucom.2021.08.115.
[5] X.Y. She, S. Dash, D. Kim, S. Mukhopadhyay, A heterogeneous spiking neural network for unsupervised learning of spatiotemporal patterns, Front. Neurosci. 14 (2021), https://doi.org/10.3389/fnins.2020.615756.
[6] C. Tan, M. Arlija, N. Kasabov, Short-term emotion recognition and understanding based on spiking neural network modelling of spatio-temporal eeg patternss, Neurocomputing 434 (2021) 137–148, https://doi.org/10.1016/j.neucom.2020.12.098.
[7] P. Lin, S. Chang, H. Wang, Q.J. Huang, J. He, Spikecd: a parameter-insensitive spiking neural network with clustering degeneracy strategy, Neural Comput. Appl. 31 (8) (2019) 3933–3945, https://doi.org/10.1007/s00521-017-3336-6.
[8] A.L. Hodgkin, A.F. Huxley, A quantitative description of membrane current and its application to conduction and excitation in nerve, J. Physiol. 117 (4) (1952) 500–544, https://doi.org/10.1113/jphysiol.1952.sp004764.
[9] R. Brette, W. Gerstner, Adaptive exponential integrate-and-fire model as an effective description of neuronal activity, J. Neurophysiol. 94 (5) (2005) 3637–3642, 10.1152/ jn.00686.
[10] E.M. Izhikevich, Simple model of spiking neurons, IEEE Trans. Neural Networks 14 (6) (2003) 1569–1572, https://doi.org/10.1109/TNN.2003.820440.
[11] F.M. Quintana, P.F. Perez, P.L. Galindo, Bio-plausible digital implementation of a reward modulated stdp synapse, Neural Computing and Applications doi:10.1007/s00521-022-07220-6.
[12] P. Stoliar, O. Schneegans, M. Rozenberg, Biologically relevant dynamical behaviors realized in an ultra-compact neuron model, Front. Neurosci. 14 (2020) 421, https://doi.org/10.3389/fnins.2020.00421.
[13] A.J. Leigh, M. Mirhassani, R. Muscedere, An efficient spiking neuron hardware system based on the hardware-oriented modified izhikevich neuron (homin) model, IEEE Trans. Circuits Syst. II Express Briefs 67 (12) (2020) 3377–3381, https://doi.org/10.1109/TCSII.2020.2984932.
[14] H.S. Wang, Endocannabinoid mediates excitatory synaptic function of β) neurexins, Front. Neurosci. 10 (3) (2016) 203, https://doi.org/10.3389/fnins.2016.00203.
[15] Z. Dargaei, X.Y. Liang, M. Serranilla, J. Santos, M.A. Woodin, Alterations in hippocampal inhibitory synaptic transmission in the r6/2 mouse model of huntington's disease, Neuroscience 404 (2019) 130–140, https://doi.org/10.1016/j.neuroscience.2019.02.007.
[16] M.S. Xue, B.V. Atallah, M. Scanziani, Equalizing excitation-inhibition ratios across visual cortical neurons, Nature 511 (7511) (2014) 596–600, https://doi.org/10.1038/nature13321.
[17] E. Giannakakis, C.E. Han, B. Weber, F. Hutchings, M. Kaiser, Towards simulations of long-term behavior of neural networks: Modeling synaptic plasticity of connections within and between human brain regions, Neurocomputing 416 (2020) 38–44, https://doi.org/10.1016/j.neucom.2020.01.050.
[18] P.U. Diehl, M. Cook, Unsupervised learning of digit recognition using spike-timing-dependent plasticity, Front. Comput. Neurosci. 9 (2015) 99, https://doi.org/10.3389/fncom.2015.00099.
[19] M.M. Poo, Towards brain-inspired artificial intelligence, Natl. Sci. Rev. 5 (6) (2018) 785, https://doi.org/10.1093/nsr/nwy120.
[20] H.A. Swadlow, Monitoring the excitability of neocortical efferent neurons to direct activation by extracellular current pulses, J. Neurophysiol. 68 (2) (1992) 605–619, https://doi.org/10.1152/jn.1992.68.2.605.
[21] M.L. Zhang, J.B. Wu, A. Belatreche, Z.H. Pan, X.R. Xie, Y.S. Chua, G.Q. Li, H. Qu, H. Z. Li, Supervised learning in spiking neural networks with synaptic delay-weight plasticity, Neurocomputing 409 (2020) 103–118, https://doi.org/10.1016/j.neucom.2020.03.079.
[22] M. Barthelemy, Morphogenesis of spatial networks, Springer, Berlin, 2018.
[23] Z. Li, T. Ren, X.Y.J., J.Y. Jin, The relationship between synchronization and percolation for regular networks, Physica A 492 (2018) 375–381. doi:10.1016/j.physa.2017.10.003.
[24] H. Lin, J.C. Wang, Percolation of a random network by statistical physics method, Int. J. Mod. Phys. C 30 (1) (2019) 1950009, https://doi.org/10.1142/S0129183119500098.
[25] L.R. Nemzer, G.D. Cravens, R.M. Worth, F. Motta, A. Placzek, V. Castro, J.Q. Lou, Critical and ictal phases in simulated eeg signals on a small-world network, Front. Comput. Neurosci. 14 (2021), https://doi.org/10.3389/fncom.2020.583350.
[26] G. Keerthana, P. Anandan, N. Nandhagopal, Enhancing the robustness and security against various attacks in a scale-free network, Wireless Pers. Commun. 117 (2021) 3029–3050, https://doi.org/10.1007/s11277-020-07356-5.
[27] D.Y. Chen, J.Y. Lu, H.C. Zhou, J.H. Jiang, P. Wu, Q.H. Guo, J.J. Ge, H.W. Zhang, K.Y. Shi, C.T. Zuo, Glucose metabolic brain network differences between chinese patients with lewy body dementia and healthy control, Behav. Neurol. 2018 (2018) 8420658, https://doi.org/10.1155/2018/8420658.
[28] D.J. Hodkinson, D. Lee, L. Becerra, D. Borsook, Scale-free amplitude modulation of low-frequency fluctuations in episodic migraine, Pain 160 (10) (2019) 2298–2304, https://doi.org/10.1097/j.pain.0000000000001619.

[29] S. Bin, G.X. Sun, C. Chen, Analysis of functional brain network based on electroencephalography and complex network, Microsyst. Technol. 27 (4) (2021) 1525–1533, https://doi.org/10.1007/s00542-019-04424-0.
[30] Y.Y. Zhang, J.C. Ren, Y.J. Qin, C. Yang, T.Y. Zhang, Q.Y. Gong, T.H. Yang, D. Zhou, Altered topological organization of functional brain networks in drug-naive patients with paroxysmal kinesigenic dyskinesia, J. Neurol. Sci. 411 (15) (2020), https://doi.org/10.1016/j.jns.2020.116702.
[31] Y.X. Zhu, T. Lu, C.M. Xie, Q. Wang, Y.J. Wang, X.J. Cao, Y.T. Su, Z. Wang, Z.J. Zhang, Functional disorganization of small-world brain networks in patients with ischemic leukoaraiosis, Front. Aging Neurosci. 12 (2020) 203, https://doi.org/10.3389/fnagi.2020.00203.
[32] G. Li, Y.D. Luo, Z.R. Zhang, Y.T. Xu, W.D. Jiao, Y.H. Jiang, S. Huang, C.W. Wang, Effects of mental fatigue on small-world brain functional network organization, Neural Plasticity 2019 (2) (2019) 1716074, https://doi.org/10.1155/2019/1716074.
[33] A. Tetereva, S. Kartashov, A. Ivanitsky, O. Martynova, Variance and scale-free properties of resting-state blood oxygenation level-dependent signal after fear memory acquisition and extinction, Front. Human Neurosci. 14 (2020), https://doi.org/10.3389/fnhum.2020.509075.
[34] J. Piersa, F. Piekniewski, T. Schreiber, Theoretical model for mesoscopic-level scale-free self-organization of functional brain networks, IEEE Trans. Neural Networks 21 (11) (2010) 1747–1758, https://doi.org/10.1109/TNN.2010.2066989.
[35] V.M. Eguiluz, D.R. Chialvo, G.A. Cecchi, M. Baliki, A.V. Apkarian, Scale-free brain functional networks, Phys. Rev. Lett. 94 (1) (2005), https://doi.org/10.1103/PhysRevLett.94.018102.
[36] Q. Zhou, D.Q. Wei, Synchronous dynamics in multilayer memristive neural networks: Effect of electromagnetic induction, IEEE Access 8 (2020) 164727–164736, https://doi.org/10.1109/ACCESS.2020.3022684.
[37] R. Zeraati, V. Priesemann, A. Levina, Self-organization toward criticality by synaptic plasticity, Front. Phys. 9 (2021), https://doi.org/10.3389/fphy.2021.619661.
[38] K.J. Wu, T.J. Wang, C.L. Wang, T.T. Du, H.W. Lu, Study on electrical synapse coupling synchronization of hindmarsh-rose neurons under gaussian white noise, Neural Comput. Appl. 30 (2) (2018) 551–561, https://doi.org/10.1007/s00521-016-2681-1.
[39] X.H. Zhang, S.Q. Liu, Stochastic resonance and synchronization behaviors of excitatory-inhibitory small-world network subjected to electromagnetic induction, Chin. Phys. B 27 (4) (2018), CNKI:SUN:ZGWL.0.2018-04-025.
[40] L. Guo, L.T. Hou, Y.X. Wu, H. Lv, H.L. Yu, Encoding specificity of scale-free spiking neural network under different external stimulations, Neurocomputing 418 (2020) 126–138, https://doi.org/10.1016/j.neucom.2020.07.11.
[41] D.J. Saunders, D. Patel, H. Hazan, H.T. Siegelmann, R. Kozma, Locally connected spiking neural networks for unsupervised feature learning, Neural Networks 119 (2019) 332–340, https://doi.org/10.1016/j.neunet.2019.08.016.
[42] L. Guo, R.X. Man, Y.X. Wu, H.L. Yu, G.Z. Xu, Anti-injury function of complex spiking neural networks under targeted attack, Neurocomputing 462 (2021) 260–271, https://doi.org/10.1016/j.neucom.2021.07.092.
[43] A. Destexhe, Z.F. Mainen, T.J. Sejnowski, An efficient method for computing synaptic conductances based on a kinetic model of receptor binding, Neural Comput. 6 (1) (1994) 14–18, https://doi.org/10.1162/neco.1994.6.1.14.
[44] S. Song, K.D. Miller, L.F. Abbott, Competitive hebbian learning through spike-timing-dependent synaptic plasticity, Nat. Neurosci. 3 (9) (2000) 919–926, https://doi.org/10.1038/78829.
[45] D. Wang, X.Z. Jin, On weighted scale-free network model with tunable clustering and congestion, Acta Phys. Sin. 61 (12) (2012), https://doi.org/10.7498/aps.61.228901.
[46] D.J. Watts, S.H. Strogatz, Collective dynamics of 'small-world' networks, Nature 393 (6684) (1998) 440–442, https://doi.org/10.1038/30918.
[47] A.L. Barabási, R. Albert, Emergence of scaling in random networks, Science 286 (1999) 509–512, https://doi.org/10.1126/science.286.5439.509.
[48] T.P. Vogels, H. Sprekeler, F. Zenke, C. Clopath, W. Gerstner, Inhibitory plasticity balances excitation and inhibition in sensory pathways and memory networks, Science 334 (6062) (2011) 1569–1573, https://doi.org/10.1126/science.1211095.
[49] R. Lyon, A computational model of filtering, detection, and compression in the cochlea, in: Proceedings of the IEEE International Conference on Acoustics, Speech, and Signal Processing 7 (1982) 1282–1285. doi:10.1109/ICASSP.1982.1171644.
[50] B. Schrauwen, J.V. Campenhout, Bsa, a fast and accurate spike train encoding scheme, in: Proceedings of the International Joint Conference on Neural Networks 4 (2003) 2825–2530. doi:10.1109/IJCNN.2003.1224019.
[51] F. Ponulak, A. Kasinski, A supervised learning in spiking neural networks with resume: sequence learning, classification, and spike shifting, Neural Comput. 22 (2) (2010) 467–510, https://doi.org/10.1162/neco.2009.11-08-901.
[52] A. Barrat, M. Barthélemy, A. Vespignani, Weighted evolving networks: coupling topology and weight dynamics, Phys. Rev. Lett. 92 (22) (2004), https://doi.org/10.1103/PhysRevLett.92.228701.
[53] I.E. Antoniou, E.T. Tsompa, Statistical analysis of weighted networks, Discrete Dynamics in Nature and Society 2008 (2008), https://doi.org/10.1155/2008/375452.

Lei Guo born in 1968, Ph.D., is a professor and deputy director with the Department of Biomedical Engineering, School of Health Science and Biomedical Engineering, Hebei University of Technology. His current research interests include neural engineering and brain-like computing.

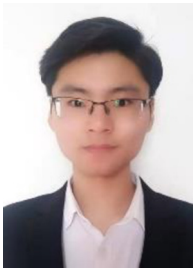

Dongzhao Liu born in 1992, B.S., is the Ph.D. candidate in the Department of Biomedical Engineering, School of Health Science and Biomedical Engineering, Hebei University of Technology. His current research interest is brain-like computing.

Youxi Wu (M'17), born in 1974, Ph.D., is a professor and director of basic teaching department of School of Artificial Intelligence, Hebei University of Technology. His current research interests include data mining and machine learning. He is a senior member of CCF.

Guizhi Xu born in 1962, Ph.D., is a professor of School of Electrical Engineering, Hebei University of Technology, and the dean of Institute of Biomedical and Health Engineering. Her current research interests include neural engineering and brain science.